The effect of intermediate layer densification on the critical current of a Bi-2223 superconducting joint

OPEN ACCESS
IOP Publishing
Superconductor Science and Technology
Supercond. Sci. Technol. **36** (2023) 035004 (10pp)
https://doi.org/10.1088/1361-6668/acaccd

The effect of intermediate layer densification on the critical current of a Bi-2223 superconducting joint

Y Takeda*, G Nishijima, K Inoue, Y Takano and H Kitaguchi

National Institute for Materials Science, 3-13 Sakura, Tsukuba, Ibaraki 305-0003, Japan

E-mail: TAKEDA.Yasuaki@nims.go.jp

Received 16 September 2022, revised 11 December 2022
Accepted for publication 19 December 2022
Published 23 January 2023

Abstract

The effect of intermediate layer densification on the critical current (I_c) of Bi-2223 superconducting joints was quantitatively studied. First, we evaluated the phase purity, density, and intergrain critical current density (J_c) of Bi-2223 thick film samples simulating the intermediate layer. The samples were uniaxially pressed to increase the film density. After two heat treatments of the pressed film, an increase in J_c was achieved. Second, we fabricated superconducting joints by synthesizing an intermediate layer between two Bi-2223 tapes. Applying a uniform uniaxial pressure on the joint resulted in the formation of a homogeneous structure. This process enables the reproducible fabrication of superconducting joints with high n values. The I_c of the superconducting joint was increased by intermediate pressing (IP) and two heat treatments. However, pressing at high pressures can mechanically damage filaments in the Bi-2223 tapes, leading to a decrease in I_c. Sample characterization showed that the optimum IP pressure range to produce high I_c was 1.5–2 $\times$ 10^8 Pa. We confirmed that pressing densified the intermediate layer of the superconducting joints. Our experimental results and analyses reveal that densification of the intermediate layer increases the I_c of Bi-2223 superconducting joints.

Keywords: superconducting joint, Bi-2223, HTS, critical current, densification

(Some figures may appear in colour only in the online journal)

1. Introduction

The commercially available Ag-sheathed multifilamentary $(Bi,Pb)_2Sr_2Ca_2Cu_3O_y$ [Bi-2223] high-temperature superconducting (HTS) tape, DI-BSCCO® [1, 2], exhibits high critical current (I_c) up to 200 A at 77 K in self-field and >500 A at 4.2 K under ~20 T parallel to the tape surface [3, 4]. This tape has been used for magnets operating at a high temperature of 20 K [2, 5, 6] and generating a high field of >24 T at around 4 K [7–9].

Superconducting joints are necessary for magnets operating in the persistent current mode [10, 11]. Persistent current mode magnets are used for magnetic resonance imaging and nuclear magnetic resonance systems because of their temporally stable magnetic field. In the last decade, significant progress on developing superconducting joints between HTS conductors has been made [11–18].

We developed a high-I_c superconducting joint between Bi-2223 tapes [13] by synthesizing a Bi-2223 intermediate layer between the exposed filaments of the two tapes. The synthesis comprises a slurry process, uniaxial pressing at room temperature, and heat treatment. It was found that the larger the number of exposed filaments of the Bi-2223 tapes, the higher the

* Author to whom any correspondence should be addressed.

I_c of the superconducting joint. To expose a large number of filaments, the Bi-2223 tapes were mechanically polished at a small angle of less than 0.4°.

In a recent study [19], I_c was improved by applying two-step sintering. The process involves an initial heat treatment, intermediate uniaxial pressing, and a second heat treatment. The superconducting joint achieved a practical I_c of 290–306 A at 4.2 K and 1 T under a resistance criterion of 10^{-9} Ω.

Although the I_c of the Bi-2223 superconducting joint has been improved, the key parameters affecting I_c have not yet been clarified. To identify these parameters, it is necessary to understand the relationships between I_c and the microstructure, density, and phase purity of the superconducting joint.

The uniaxial pressing pressure on the Bi-2223 intermediate layer significantly influences the microstructure and density, as demonstrated in bulk samples [20–22] and thick films [23]. During the joining process we applied intermediate pressing (IP) pressure of about 200 MPa [19], which likely densified the intermediate layer. However, the effect of densification has not yet been quantitatively evaluated.

In this study, we clarify the effect of intermediate layer densification achieved by IP on the I_c of the Bi-2223 superconducting joint. Firstly, we evaluated the phase purity, density, and intergrain critical current density (J_c) of thick film samples. The relationship between density and intergrain J_c was established. Secondly, the fabrication process of the superconducting joint was modified to achieve a uniform uniaxial pressure. The relationships between the IP pressure, density of the intermediate layer, and I_c of the superconducting joints were determined.

2. Relationship between density and J_c of thick film samples

2.1. Experimental

Thick film samples simulating the intermediate layer of a Bi-2223 superconducting joint were prepared by a slurry process [23]. Figure 1 shows a schematic of the sample and flow chart of the sample preparation process. Commercially available Bi-2223 precursor powder produced by TEP Co., Ltd was used. The nominal chemical composition of the powder was Bi:Pb:Sr:Ca:Cu = 1.6:0.45:1.9:2.0:3.0. The slurry was obtained by mixing the precursor powder with EtOH/1-BuOH solvent.

The slurry was dropped onto a Ag sheet and dried in air. The Ag sheet was 15 mm long, 5 mm wide, and 0.2 mm thick. The dried samples were uniaxially pressed at 2.0×10^8 Pa (about 200 MPa). Sample TF1 was prepared at this stage as shown in figure 1(b). The other pressed films were each covered with a 30 μm thick Ag foil. We performed the first heat treatment (HT1) for these films. At this stage, sample TF2 was ready. We carried out the second heat treatment (HT2) for the remaining samples after IP to prepare sample TF3–5. IP pressures (P_{IP}) for samples TF3–5 are shown in table 1. HT conditions for both HT1 and HT2 were at 815 °C for 36 h under a partial

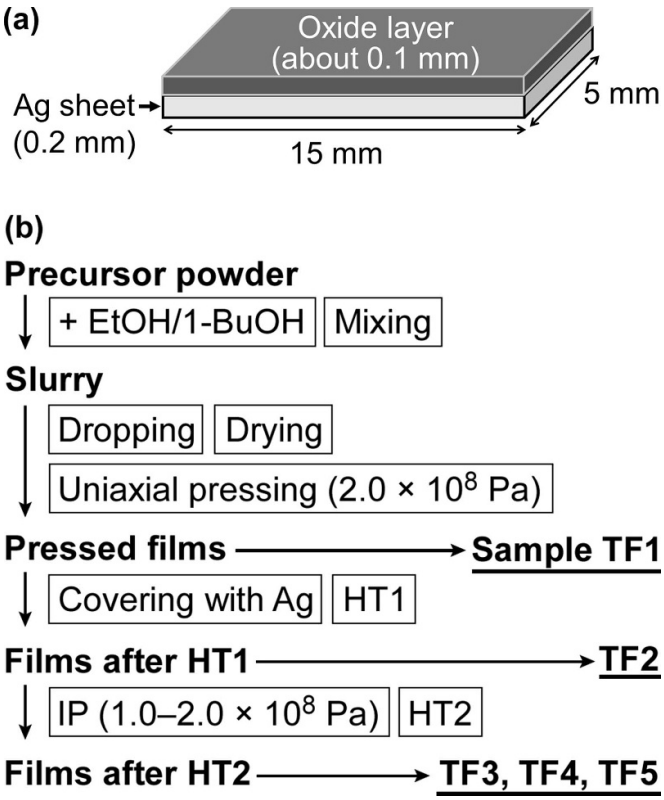

Figure 1. (a) Schematic of the thick film sample and (b) sample preparation flow chart.

oxygen pressure (P_{O2}) of 3 kPa in a tube furnace. We controlled P_{O2} by flowing 3%O_2/Ar gas in the furnace. The thickness of the oxide layer of the obtained samples was about 0.1 mm. The Ag foil and sheet were removed as needed during characterization.

The density (ρ) of the samples was calculated using the mass and dimensions of the rectangular oxide layer after removing the Ag foil and sheet. The theoretical density of 6.3 g cm^{-3} [24] was used to calculate the relative density (D).

$\theta/2\theta$ surface x-ray diffraction measurements were performed using a Rigaku MiniFlex II. The measurements were performed on the surface of the oxide layer and the oxide/Ag interface. The molar fraction of the Bi-2223 phase ($f_{\text{Bi-2223}}$) was estimated by

$$f_{\text{Bi-2223}} = \frac{I_{\text{Bi-2223}}}{I_{\text{Bi-2223}} + I_{\text{Bi-2212}}} \quad (1)$$

where $I_{\text{Bi-2223}}$ and $I_{\text{Bi-2212}}$ are the integrated intensities for the 00$\underline{14}$(Bi-2223) peak with 2θ of about 34° and 00$\underline{12}$(Bi-2212 [$(Bi,Pb)_2Sr_2CaCu_2O_y$]) peak with 2θ of about 35° in the x-ray diffraction pattern.

The intergrain J_c for the samples was evaluated at 77 K and zero external field by remanent magnetization measurements [23, 25] using a SQUID magnetometer (MPMS, Quantum Design). We used the extended Bean model to calculate J_c. The magnetic field was applied normal to the surface of the samples, i.e. parallel to the pressing direction.

Table 1. Thick film sample specifications. Heat treatment conditions for both HT1 and HT2 were at a partial oxygen pressure (P_{O2}) of 3 kPa and 815 °C for 36 h.

Sample	Heat treatment and IP	P_{IP} / 10^8 Pa	$f_{Bi\text{-}2223}$ / −(Surface)	$f_{Bi\text{-}2223}$ / −(Interface)	ρ / g cm^{-3}	D / %	Intergrain J_c / kA cm^{-2} (77 K, zero external field)
TF1	—	—	0.094	—	3.90	62	—
TF2	HT1	—	0.769	0.853	3.62	57	0.25
TF3	HT1 → IP → HT2	1.0	0.883	0.902	3.86	61	1.1
TF4	HT1 → IP → HT2	1.5	0.932	0.886	4.02	64	1.4
TF5	HT1 → IP → HT2	2.0	0.891	0.884	4.21	67	1.8

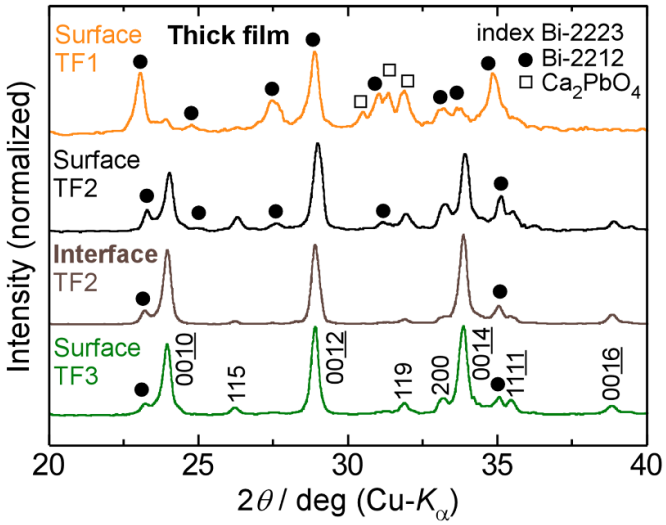

Figure 2. Typical surface x-ray diffraction patterns of sample TF1–3. The Bi-2223 phase formation progressed significantly during HT1. In the oxide/Ag interface of TF2, Bi-2223 was the main phase. Bi-2223 was the main phase even on the oxide surface of TF3.

2.2. Results

Figure 2 shows typical surface x-ray diffraction patterns for the samples. The main phase of TF1 was Bi-2212. There were also small amounts of Bi-2223 and Ca_2PbO_4 phases. Although CuO or (Ca,Sr)-Cu-O phases should also exist on the oxide surface considering the nominal chemical composition, we could not clearly find their peaks. This is probably because of the overlapping peaks, their scarce amount, or small crystallite size.

The Bi-2223 phase formation progressed significantly during HT1. The unreacted Bi-2212 phase remained on the oxide surface of sample TF2, whereas Bi-2223 was the main phase in the oxide/Ag interface. It is well known that the presence of Ag aids in the formation and *c*-axis grain alignment of the Bi-2223 phase [26, 27]. The diffraction pattern in the interface of TF2 indicates improved Bi-2223 phase formation and *c*-axis grain alignment. Even on the surface of TF3, Bi-2223 was the main phase.

Table 1 summarizes the $f_{Bi\text{-}2223}$ values for the surface and interface, ρ, D, and the intergrain J_c for sample TF1–5. For TF3–5, $f_{Bi\text{-}2223}$ values were not dependent on P_{IP} and larger than 0.88 on both the surface and interface. This indicates that Bi-2223 was the main phase for the entire sample after HT2. $f_{Bi\text{-}2223}$ on the interface of TF2 was 0.853, which is larger than that on the oxide surface and comparable to that for TF3–5 because of the presence of Ag.

The ρ of TF1 was 3.90 g cm^{-3}, which corresponds to a D of 62%. This relatively low value was probably due to the insufficient pressing pressure of 2.0 × 10^8 Pa. TF2 had a lower ρ of 3.62 g cm^{-3}. This is because the oxide layer swelled during HT1 when the Bi-2223 phase was being formed [28, 29].

In preliminary experiments, we obtained higher ρ of 4.5 g cm^{-3} in a thick film by high-pressure pressing at 1.0 × 10^9 Pa (about 1 GPa) before HT1. Due to the swelling, however, ρ of this thick film decreased to 3.7 g cm^{-3}, which is comparable to that of TF2. This indicates that it is difficult to improve final ρ of thick films by high-pressure pressing before HT1.

ρ increased after IP and HT2. IP contributed to the densification, as demonstrated in a bulk sample [21]. In the present work, it was found that the higher the P_{IP}, the higher the ρ of the Bi-2223 thick film. Among all samples, the highest ρ of 4.21 g cm^{-3} corresponding to a D of 67% was obtained by TF5. This ρ value is comparable to that for bulk samples prepared with a P_{IP} of 1–2 × 10^8 Pa [21, 22]. However, this ρ value is still low compared with that of the filaments of the Bi-2223 tape (D of about 100%) fabricated by rolling and overpressure sintering processes [2].

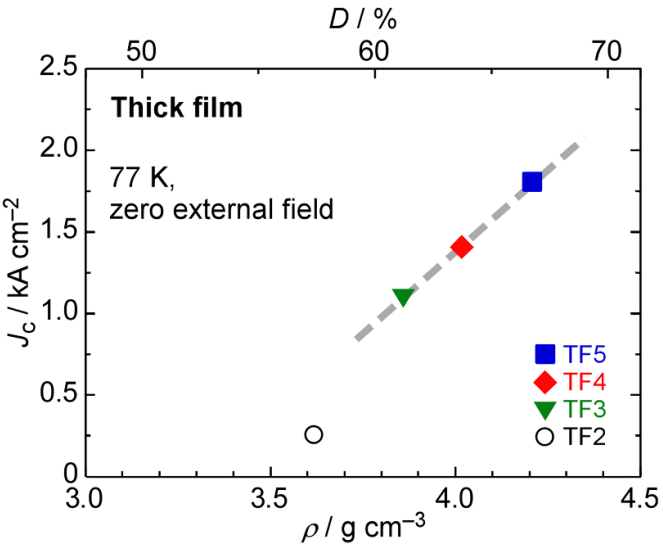

Figure 3. Relationship between ρ and intergrain J_c at 77 K and zero external field for sample TF2–5. The gray dashed line was derived from TF3–5 data points using the least-squares method. J_c increased after IP and HT2. In the thick film, an increase in intergrain J_c is achieved by densification.

Figure 3 shows the relationship between ρ and intergrain J_c at 77 K and zero external field for TF2–5. The gray dashed line was derived from TF3–5 data points using the least-squares method. J_c increased after IP and HT2. This increase in J_c is mainly due to the high purification and densification. There appears to be a linear relationship between ρ and J_c in TF3–5. Therefore, it was verified that in the Bi-2223 thick film, an increase in intergrain J_c is achieved by densification.

3. I_c and microstructure evaluation for superconducting joint samples

3.1. Experimental

DI-BSCCO® Type H tapes 4.2 mm wide and 0.22 mm thick (without mechanical reinforcements) were used to fabricate the Bi-2223 superconducting joints. Figure 4(a) shows the transverse cross-sectional view and height profile of one side of the Bi-2223 tape. This cross-section shows a bulge, i.e., the center is thicker than that of the edges. Height profile measurements in the lateral direction (x) using a laser microscope (Keyence VK-X1100/1000SP1976) showed that the height of the center ($x = 2$ mm) was about 20 μm larger than that of the edges.

The uniaxial pressure on the joint will not be uniform using such tapes, i.e., the high pressure is concentrated in the thicker central part. This non-uniform pressure distribution is one of the major reasons why the densification demonstrated in the thick film could not be replicated in the intermediate layer of a joint.

To ensure that the applied uniaxial pressure is uniform, the tape was flattened by polishing both sides. Figure 4(b) shows the transverse cross-sectional view and height profile of one side of the flattened Bi-2223 tape. The thickness of the center

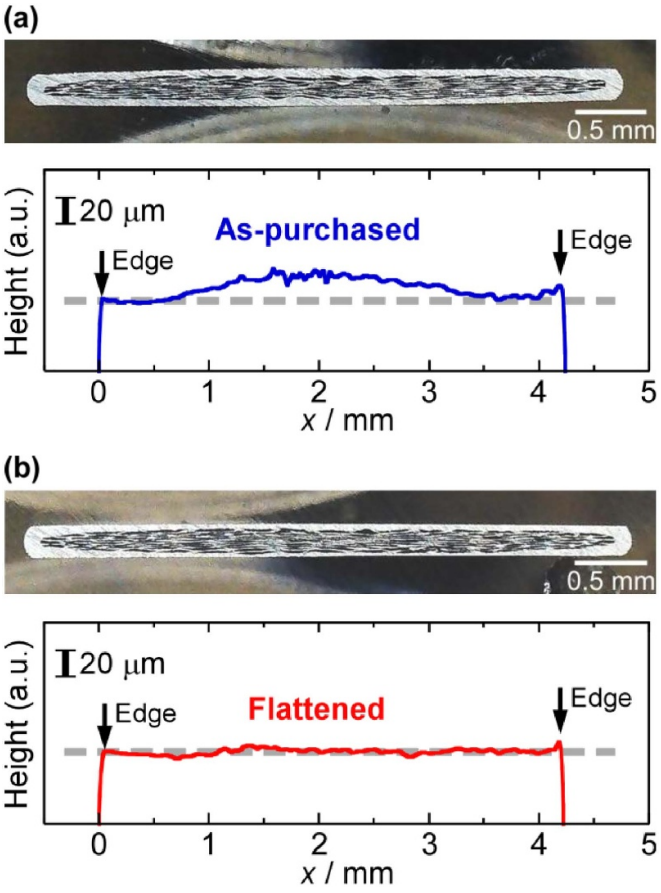

Figure 4. Transverse cross-sectional view and height profile of one side in the lateral direction (x) for (a) as-purchased Bi-2223 tape and (b) flattened Bi-2223 tape. The gray dashed line in the height profiles is the reference level. The surface of the flattened tape is perfectly flat.

of the flattened tape was 30–40 μm smaller than that of the as-purchased tape. Height profile measurements show that the surface of the flattened tape is perfectly flat.

In the present work, straight lap joint samples were fabricated using flattened Bi-2223 tapes 6 cm long. Figure 5(a) shows a schematic of the joint. One end of each flattened tape was polished at 0.3° to expose most filaments [13, 19]. The joining procedure involving Bi-2223 intermediate layer synthesis was similar to that described in [13, 19] and was applied using the same slurry to prepare the thick film samples.

We confirmed that the uniaxial pressure in pressing could be made uniform using the flattened tapes, as shown in figure 5(b). Joint samples using as-purchased tapes or flattened tapes were prepared and pressed at 1.0–2.0 $\times$ 10^8 Pa with the pressure measurement films (Fujifilm Prescale HS). The sample using the as-purchased tapes showed a color gradient at 1.0 $\times$ 10^8 Pa. This indicates that the high pressure is concentrated in the thicker central part and the thinner edges are not pressed. Even when pressing at 2.0 $\times$ 10^8 Pa, although the pressed area increased due to sample deformation, the thinner edges are still not pressed. In contrast, the joint using the flattened tapes showed no color gradient despite the pressing pressure. This indicates the uniform pressure distribution at

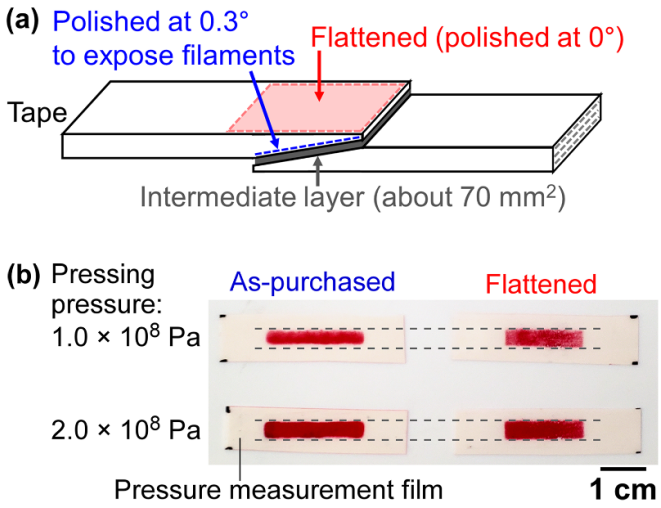

Figure 5. (a) Schematic of the straight lap joint using the flattened tapes. (b) Photograph of pressure measurement films (Fujifilm Prescale HS). Joints using the as-purchased tapes or flattened tapes were pressed at 1.0–2.0 $\times$ 10^8 Pa with the pressure measurement films. These films indicate that uniaxial pressure in pressing can be made uniform by using the flattened tapes.

1.0–2.0 $\times$ 10^8 Pa. The width of the region to which pressure was applied almost completely corresponded to that of the tape (4.2 mm).

The intermediate layer area was about 70 mm^2. However, there was an area uncertainty of about 10%. This means that the uncertainty of the pressing pressure was also about 10%. The joint was uniaxially pressed at (2.0 $\pm$ 0.2) $\times$ 10^8 Pa before HT1. HT2 was performed for some samples after IP at a P_{IP} of 1–2 $\times$ 10^8 Pa with $\pm$10% uncertainty. HT conditions were the same as those for the fabrication of the thick film samples, i.e., at P_{O2} of 3 kPa and 815 °C for 36 h.

Transport measurements in the self-field were performed for the samples in a liquid nitrogen bath (77 K). The conventional dc four-probe method was used. I_c was determined at a voltage of $V = 0.2$ μV. Assuming an empirical power law model ($V \propto I^n$), the exponent n was calculated for a voltage range of 0.2 μV $\leqslant V \leqslant$ 0.7 μV.

The microstructures of the samples were observed using a field emission scanning electron microscope, Hitachi SU-70. Secondary electron images were obtained from the polished surface of the transverse cross-section of the samples. We estimated the filling factor (F) for the intermediate layer of the samples by image analysis. More than ten images of the intermediate layer were obtained for each sample. The size of the images was 25 μm $\times$ 18 μm. We estimated F values by image thresholding, measuring F for each image, and calculating the mean and standard deviation values.

3.2. Results

3.2.1. I_c and n values after HT1. Eight sample joints were fabricated. Table 2 summarizes the I_c, n and P_{IP} for each sample. Samples J1 and J2 were prepared using only HT1 (without IP). For J3–8, the I_c and n values after HT2 were also evaluated.

Table 2. Joint sample specifications. I_c and n values at 77 K in self-field were examined by transport measurements. The heat treatment conditions were at P_{O2} = 3 kPa and 815 °C for 36 h.

	After HT1			After HT2	
Sample	I_c / A	n / –	P_{IP}[a] / 10^8 Pa	I_c / A	n / –
J1	37.3	14.1	— (only HT1)		
J2	31.6	15.2	— (only HT1)		
J3	33.8	18.1	1.0	40.3	17.6
J4	42.6	13.1	1.5	73.1	11.5
J5	39.3	15.7	1.5	68.7	15.2
J6	24.7	18.9	2.0	73.3	16.3
J7	33.8	16.5	2.0	45.1	8.35
J8	22.8	16.5	2.0	5.1	8.63

[a] P_{IP} uncertainty was about 10%.

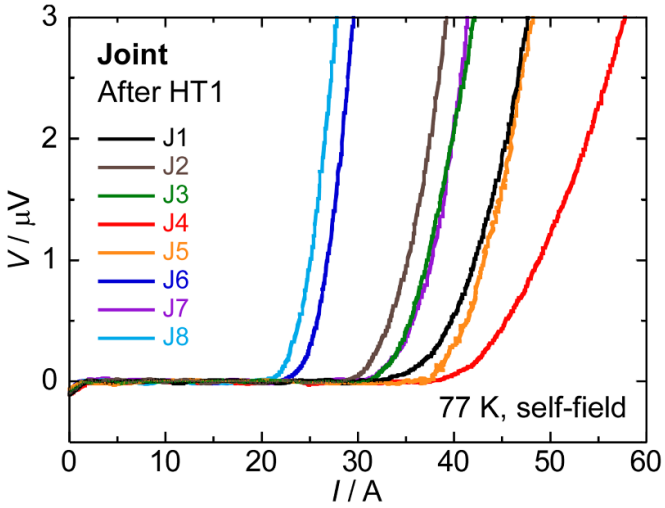

Figure 6. *V–I* curves measured at 77 K in the self-field for sample J1–8 after HT1. All curves show a typical superconducting to normal transition, indicating that the superconducting joints were formed in all samples after HT1.

Figure 6 shows the *V–I* curves at 77 K in the self-field for the samples after HT1. All *V–I* curves show a typical superconducting to normal transition, indicating that superconducting joints were formed in all samples after HT1. As shown in table 2, the ranges of I_c and n values were 22.8–42.6 A and 13.1–18.9, respectively. In the previously reported superconducting joints, the n values were 6–10 [13, 19]. In this study, after HT1, the samples exhibited higher n values with high reproducibility.

The higher n values are attributed to the homogenous structure [10], as demonstrated in Nb-Ti wires and Bi-2223 tapes [30, 31]. By using flattened Bi-2223 tapes, a uniform pressing pressure could be applied enabling the formation of a homogeneous structure. This allows the reproducible fabrication of superconducting joints possessing high n values.

3.2.2. Increase in I_c after IP and HT2. In a previous study, we demonstrated I_c improvement in the superconducting joint

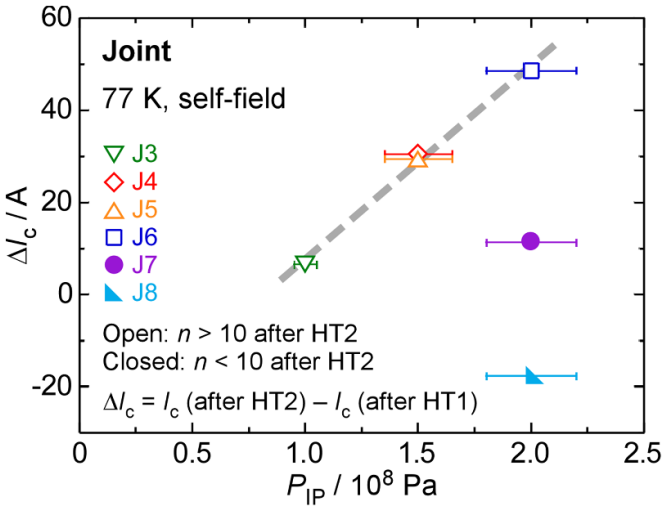

Figure 7. Relationship between P_{IP} and ΔI_c at 77 K in self-field for sample J3–8. The P_{IP} error bars correspond to $\pm 10\%$ uncertainty. The gray dashed line was derived from J3–6 data points by the least-squares method. There appears to be a linear relationship between P_{IP} and ΔI_c of these samples. At a P_{IP} of 2.0×10^8 Pa, a large ΔI_c was not reproduced.

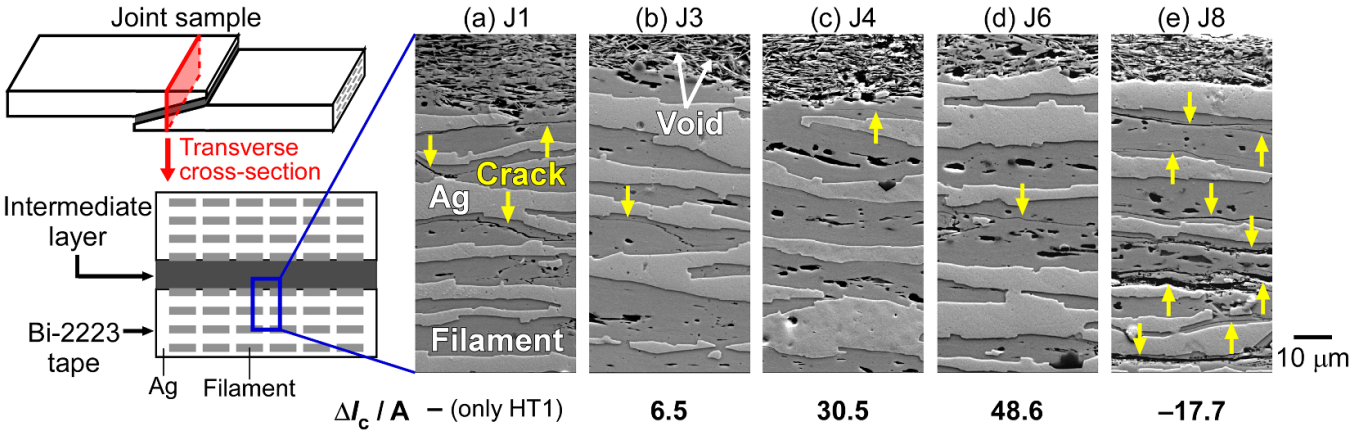

Figure 8. Secondary electron images of typical polished surfaces for the joining part of J1, J3, J4, J6, and J8. The position for the observation and ΔI_c of each sample are also shown. Many cracks were observed in most J8 filaments. IP at a P_{IP} of 2.0×10^8 Pa can cause significant damage to the filaments in the Bi-2223 tape, resulting in the small ΔI_c.

by introducing IP and HT2 [19]. In this study, in order to quantify the increase in I_c, we used increments of I_c, $\Delta I_c = I_c$ (after HT2) $- I_c$ (after HT1). The relationship between P_{IP} and ΔI_c for J3–8 is shown in figure 7. The P_{IP} error bars correspond to $\pm 10\%$ uncertainty. The gray dashed line was derived from J3–6 data points by the least-squares method.

The n values for J3–6 were >11 after HT2, as shown in table 2. There appears to be a linear relationship between P_{IP} and ΔI_c for these samples. This implies that a denser intermediate layer was formed with a higher P_{IP}, resulting in a larger ΔI_c. J6 at a P_{IP} of 2.0×10^8 Pa showed the largest ΔI_c of 48.6 A.

The ΔI_c of J7 and J8 were much smaller than that of J6. The P_{IP} for J7 and J8 were similar to that for J6. A large ΔI_c was not reproduced at a P_{IP} of 2.0×10^8 Pa. As shown in table 2, J7 and J8 had low n values (<9) after HT2. The cause of the small ΔI_c and low n values for J7 and J8 is discussed in the next section.

The ΔI_c of J3 at a P_{IP} of 1.0×10^8 Pa was only 6.5 A. This may be because the densification of the intermediate layer was insufficient to achieve a large ΔI_c. At a P_{IP} of 1.5×10^8 Pa, relatively large ΔI_c of 29.4 and 30.5 A were observed in J4 and J5, respectively. There is an optimum P_{IP} of around $1.5–2 \times 10^8$ Pa to achieve a large ΔI_c with high reproducibility.

3.2.3. Evaluation of microstructure and intermediate layer densification. The microstructures of J1, J3, J4, J6 and J8 were examined. An intermediate layer with a homogeneous thickness of about 30 μm is formed in each sample, as reported in [19]. Figure 8 shows typical secondary electron images of the polished surfaces of the samples. In each image, the upper and lower parts correspond to the intermediate layer and Bi-2223 tape, respectively. As reported in [13, 19], the grains were in good contact at the interfaces

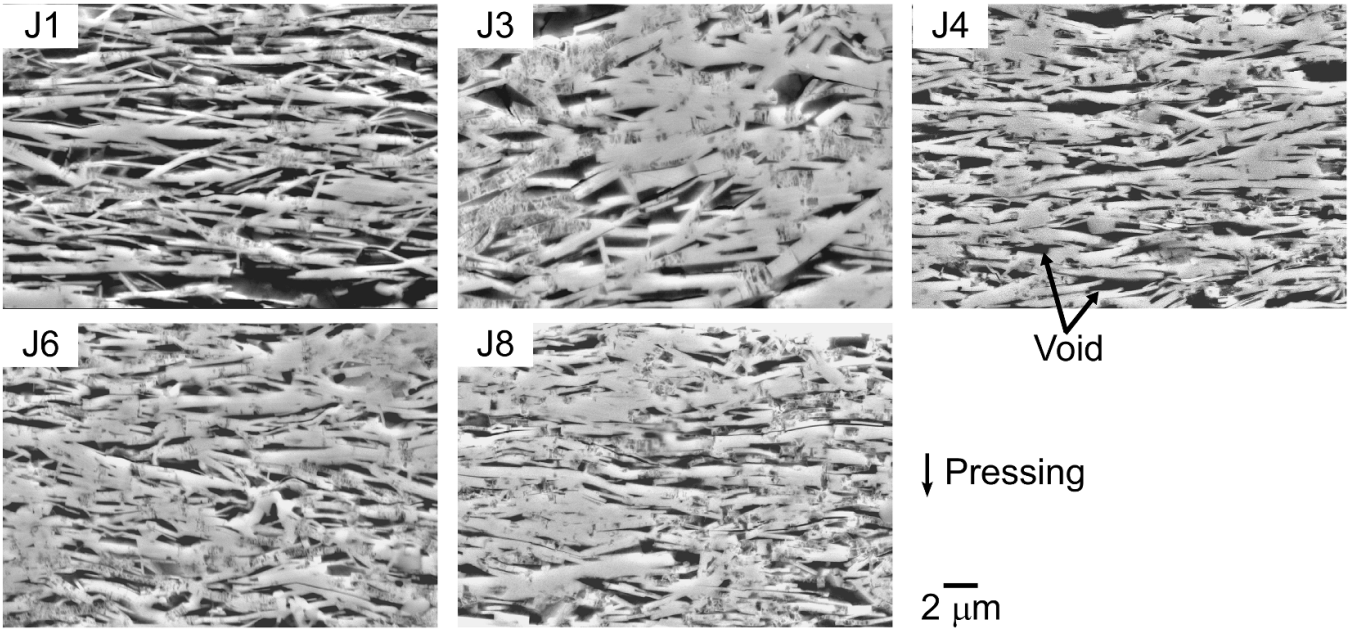

Figure 9. Typical secondary electron images of polished surfaces for the intermediate layers of J1, J3, J4, J6 and J8. The filling factor (F) of the intermediate layer was calculated using such images.

between the intermediate layer and filaments. A large number of voids were observed in the intermediate layer of each sample.

As shown in figure 8(e), many cracks were observed in most filaments of J8. Few and thin cracks were observed in the filaments of the other samples. There was a difference in the damage to the filaments between J6 and J8 pressed at a P_{IP} of 2.0 $\times$ 10^8 Pa. This may be due to the uncertainty of P_{IP}. The actual P_{IP} applied to J8 was probably higher than the nominal value, resulting in significant damage to the filaments.

Figure 9 shows typical secondary electron images of the polished surface of the intermediate layer for J1, J3, J4, J6, and J8. General plate-like Bi-2223 grains were found in each sample. The grain size was 5–10 μm, which was comparable to that of the previously reported bulks heat-treated at P_{O2} = 3 kPa and 815 °C–825 °C [22].

In J3, J4, J6, and J8, the main phase of the intermediate layer was Bi-2223, which was not dependent on P_{IP}. This result is consistent with that of the thick film samples shown in section 2.2. We could not find coarse impurities such as $(Pb,Bi)_3Sr_2Ca_2CuO_y$ (Pb-3221), Bi-2212, or (Ca,Sr)-Cu-O phases in the intermediate layer.

There appeared to be no difference in the degree of c-axis grain alignment among these samples. The c-axis grain misorientation angle for the intermediate layer of each sample was estimated from the directions of the plate-like Bi-2223 grains. Although there was broad distribution of the misorientation angle depending on the observation location, the mean misorientation angle was about 15°–30° calculated using about 30 grains in each sample. This suggests that a weakly grain-oriented intermediate layer was formed in each sample because pressing pressure up to 2.0 $\times$ 10^8 Pa was too low to promote c-axis grain alignment.

Table 3. P_{IP} and calculated F of the intermediate layer with mean and standard deviation values.

Sample	P_{IP}[a] / 10^8 Pa	F / %
J1	— (only HT1)	68.6 ± 3.0
J3	1.0	71.2 ± 2.2
J4	1.5	73.7 ± 1.9
J6	2.0	77.4 ± 2.0
J8	2.0	78.0 ± 1.9

[a] P_{IP} uncertainty was about 10%.

The calculated filling factors (F) with the mean and standard deviation values for the intermediate layer of each sample are summarized in table 3. The table quantitatively shows that IP densifies the intermediate layer. The higher P_{IP}, the denser the intermediate layer.

The F value of J8 is comparable to that of J6. This means that the densification by IP was achieved even in the intermediate layer of J8, although the ΔI_c of J8 was much smaller than that of J6. It has been reported that mechanical damage to the filaments deteriorates the I_c and n values of Bi-2223 tape [32, 33]. The filaments in J8 were significantly damaged as shown in figure 8(e), resulting in the lowered ΔI_c and n values.

Although the microstructure of J7 (P_{IP} of 2.0 $\times$ 10^8 Pa) was not observed because J7 was degraded after the transport measurements, the corresponding F value is probably similar to that of J6 and J8. The small ΔI_c and low n value of J7 was probably caused by the damage to the filaments in the Bi-2223 tapes.

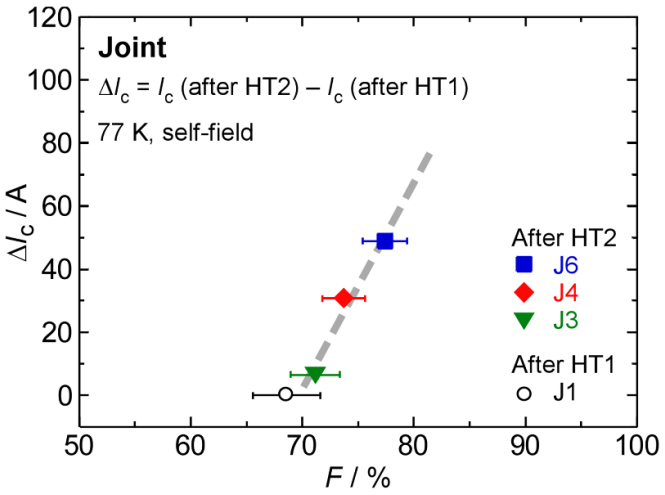

Figure 10. Relationship between F and ΔI_c for the superconducting joint samples J1, J3, J4 and J6. Gray dashed line was derived from J3, J4, and J6 data points using the least-squares method. ΔI_c appears to be positively correlated with F, indicating that the densification of the intermediate layer produces a large ΔI_c of the Bi-2223 superconducting joint.

4. Discussion

4.1. Relationship between intermediate layer densification and ΔI_c of the superconducting joint

As presented in section 2.2, IP increased the ρ of the thick film samples. The higher the P_{IP}, the higher the ρ in sample TF3–5. An increase in intergrain J_c was achieved by the densification. Assuming that J_c of TF2 is a typical value for a thick film after HT1, increments of J_c, $\Delta J_c = J_c$ (after HT2) $- J_c$ (after HT1) will also increase by the densification in TF3–5.

In the superconducting joints, IP densified the intermediate layer, as shown in table 3. The higher the P_{IP}, the higher the F in samples J3, J4, and J6. This densification of the intermediate layer contributed to the large ΔI_c of the superconducting joint.

Figure 10 shows the relationship between F and ΔI_c for the superconducting joint samples J1, J3, J4, and J6. J1, which was prepared with only one HT process (HT1), was plotted as $\Delta I_c = 0$. The gray dashed line was derived from J3, J4, and J6 data points using the least-squares method. ΔI_c appears to be positively correlated with F. It can be concluded that the densification of the intermediate layer produces a large ΔI_c in the Bi-2223 superconducting joint.

4.2. Achieving high I_c in the Bi-2223 superconducting joint

We clarified that the density of the intermediate layer is one of the key parameters affecting I_c of the Bi-2223 superconducting joint. Figure 10 suggests that if the intermediate layer density is increased to $F > 90\%$, a ΔI_c above 120 A can be achieved. Given that the I_c of the joints after HT1 ranged from 22.8 to 42.6 A, an I_c above 140 A is possible after HT2 with a very dense intermediate layer. This I_c is comparable to that of the commercially available Bi-2223 tape [2].

High-pressure IP can cause mechanical damage to the filaments in Bi-2223 tapes, and densification methods other than uniaxial pressing are needed to obtain dense intermediate layers. Hot pressing, which has been demonstrated in Bi-2223 tapes [34], may be effective. However, filament damage can occur and needs to be suppressed. It may be possible to introduce an already very dense material prepared in advance as an intermediate layer. However, achieving good grain contact at the joining interface may be difficult.

The large ΔI_c demonstrated in this study is attributed to the increase in intergrain J_c of the intermediate layer due to densification. Other methods for controlling the J_c of the intermediate layer can be effective in producing a high I_c. The significant parameters for controlling J_c include constituent phase [2], c-axis grain alignment [35], chemical composition [22, 23], and grain boundary structure [36]. Among them, improving c-axis grain alignment is promising because the grain alignment of the intermediate layer was poor, as shown in 3.2.3.

5. Conclusion

We clarified the effect of Bi-2223 intermediate layer densification achieved by IP on the I_c of Bi-2223 superconducting joints. The following conclusions are drawn:

(a) Bi-2223 thick films can be densified by IP. An increase in intergrain Jc can be achieved by densification.
(b) Using flattened Bi-2223 tapes for making a joint enables uniform uniaxial pressure to be applied. The uniform pressure probably promotes the formation of a homogeneous structure. This allows the reproducible fabrication of superconducting joints with high n values.
(c) The I_c of Bi-2223 superconducting joints could be increased by applying IP and HT2. However, the filaments of the Bi-2223 tapes can be damaged by high-pressure IP, which then causes I_c deterioration in the joint. To achieve a high I_c the optimum P_{IP} is in the range of 1.5–2 $\times$ 10^8 Pa.
(d) The densification of the Bi-2223 intermediate layer by IP increases the ΔI_c of the superconducting joint. The density of the intermediate layer is a key parameter affecting the I_c of the Bi-2223 superconducting joint.
(e) In order to further enhance the I_c of Bi-2223 superconducting joints, densification methods other than uniaxial pressing are needed. Controlling J_c of the intermediate layer is also effective in producing a high I_c.

Data availability statement

The data that support the findings of this study are available upon reasonable request from the authors.s.

Acknowledgments

This work was supported by JST Mirai-Program Grant Nos. JPMJMI17A2 and JSPS KAKENHI Grant No. JP22K14482, Japan.

ORCID iDs

Y Takeda https://orcid.org/0000-0001-7217-9853
G Nishijima https://orcid.org/0000-0001-7493-0559

References

[1] Ayai N *et al* 2008 DI-BSCCO wire with I_c over 200 A at 77 K *J. Phys.: Conf. Ser.* **97** 012112
[2] Sato K, Kobayashi S and Nakashima T 2012 Present status and future perspective of bismuth-based high-temperature superconducting wires realizing application systems *Jpn. J. Appl. Phys.* **51** 010006
[3] Miyoshi Y, Nishijima G, Kitaguchi H and Chaud X 2015 High field I_c characterizations of commercial HTS conductors *Physica* C **516** 31–35
[4] Bonura M, Barth C and Senatore C 2019 Electrical and thermo-physical properties of Ni-alloy reinforced Bi-2223 conductors *IEEE Trans. Appl. Supercond.* **29** 6400205
[5] Kusada S *et al* 2007 The project overview of the hts magnet for superconducting maglev *IEEE Trans. Appl. Supercond.* **17** 2111–6
[6] Terao Y *et al* 2013 Newly designed 3 T MRI magnet wound with Bi-2223 tape conductors *IEEE Trans. Appl. Supercond.* **23** 4400904
[7] Hashi K *et al* 2015 Achievement of 1020 MHz NMR *J. Magn. Reson.* **256** 30–33
[8] Nishijima G *et al* 2016 Successful upgrading of 920-MHz NMR superconducting magnet to 1020 MHz using Bi-2223 innermost Coil *IEEE Trans. Appl. Supercond.* **26** 4303007
[9] Awaji S, Watanabe K, Oguro H, Miyazaki H, Hanai S, Tosaka T and Ioka S 2017 First performance test of a 25 T cryogen-free superconducting magnet *Supercond. Sci. Technol.* **30** 065001
[10] Brittles G D, Mousavi T, Grovenor C R M, Aksoy C and Speller S C 2015 Persistent current joints between technological superconductors *Supercond. Sci. Technol.* **28** 093001
[11] Takeda Y, Maeda H, Ohki K and Yanagisawa Y 2022 Review of the temporal stability of the magnetic field for ultra-high field superconducting magnets with a particular focus on superconducting joints between HTS conductors *Supercond. Sci. Technol.* **35** 043002
[12] Park Y, Lee M, Ann H, Choi Y H and Lee H 2014 A superconducting joint for $GdBa_2Cu_3O_{7-\delta}$-coated conductors *NPG Asia Mater.* **6** e98
[13] Takeda Y, Motoki T, Kitaguchi H, Nakashima T, Kobayashi S, Kato T and Shimoyama J 2019 High I_c superconducting joint between Bi2223 tapes *Appl. Phys. Express* **12** 023003
[14] Ohki K *et al* 2017 Fabrication, microstructure and persistent current measurement of an intermediate grown superconducting (iGS) joint between REBCO-coated conductors *Supercond. Sci. Technol.* **30** 115017
[15] Chen P *et al* 2017 Development of a persistent superconducting joint between Bi-2212/Ag-alloy multifilamentary round wires *Supercond. Sci. Technol.* **30** 025020
[16] Mukoyama S, Nakai A, Sakamoto H, Matsumoto S, Nishijima G, Hamada M, Saito K and Miyoshi Y 2018 Superconducting joint of REBCO wires for MRI magnet *J. Phys.: Conf. Ser.* **1054** 012038
[17] Jin X, Suetomi Y, Piao R, Matsutake Y, Yagai T, Mochida H, Yanagisawa Y and Maeda H 2019 Superconducting joint between multi-filamentary $Bi_2Sr_2Ca_2Cu_3O_{10+\delta}$ tapes based on incongruent melting for NMR and MRI applications *Supercond. Sci. Technol.* **32** 035011
[18] Mousavi T, Santra S, Melhem Z, Speller S and Grovenor C 2021 Superconducting joint structures for Bi-2212 wires using a powder-in-tube technique *IEEE Trans. Appl. Supercond.* **31** 6400504
[19] Takeda Y *et al* 2022 Critical current improvement and resistance evaluation of superconducting joint between Bi2223 tapes *Supercond. Sci. Technol.* **35** 02LT02
[20] Asano T, Tanaka Y, Fukutomi M, Jikihara K, Machida J and Maeda H 1988 Preparation of highly oriented microstructure in the (Bi, Pb)-Sr-Ca-Cu-O Sintered Oxide Superconductor *Jpn. J. Appl. Phys.* **27** L1652–4
[21] Ito A, Matsuda M, Iwai Y, Ishii M, Takata M, Yamashita T and Koinuma H 1989 Influence of intermediate pressing on superconducting characteristics in Bi-Pb-Sr-Ca-Cu-O System *Jpn. J. Appl. Phys.* **28** L380–1
[22] Takeda Y, Shimoyama J, Motoki T, Kishio K, Nakashima T, Kagiyama T, Kobayashi S and Hayashi K 2017 Fabrication of Bi2223 bulks with high critical current properties sintered in Ag tubes *Physica* C **534** 9–12
[23] Takeda Y, Shimoyama J, Motoki T, Nakamura S, Nakashima T, Kobayashi S and Kato T 2018 Development of high J_c Bi2223/Ag thick film materials prepared by heat treatment under low P_{O2} *Supercond. Sci. Technol.* **31** 074002
[24] Hu Q Y, Liu H K and Dou S X 1996 Effect of mechanical deformation on the mass density of Ag-clad $(Bi,Pb)_2Sr_2Ca_2Cu_3O_{10}$ wire and tape *Appl. Supercond.* **4** 17–24
[25] Müller K-H, Andrikidis C, Du J, Leslie K E and Foley C P 1999 Connectivity and limitation of critical current in Bi-Pb-Sr-Ca-Cu/Ag tapes *Phys. Rev.* B **60** 659–66
[26] Flükiger R, Grasso G, Grivel J C, Marti F, Dhallé M and Huang Y 1997 Phase formation and critical current density in Bi,Pb(2223) tapes *Supercond. Sci. Technol.* **10** A68–A92
[27] Zhang L, Mironova M, Selvamanickam V and Salama K 2000 Study of Ag/BSCCO interface in Ag-sheathed multifilament Bi-2223 tapes *Physica* C **341–348** 1471–2
[28] Jiang J, Cai X Y, Polyanskii A A, Schwartzkopf L A, Larbalestier D C, Parrella R D, Li Q, Rupich M W and Riley J G N 2001 Through-process study of factors controlling the critical current density of Ag-sheathed $(Bi,Pb)_2Sr_2Ca_2Cu_3O_x$ tapes *Supercond. Sci. Technol.* **14** 548–56
[29] Kato T *et al* 2004 Development of high performance Ag sheathed Bi2223 wire *Physica* C **412–414** 1066–72
[30] Ekin J W 1987 Irregularity in Nb-Ti filament area and electric field *versus* current characteristics *Cryogenics* **27** 603–7
[31] Rimikis A, Kimmich R and Schneider T 2000 Investigation of *n*-values of Composite Superconductors *IEEE Trans. Appl. Supercond.* **10** 1239–42
[32] Ochiai S, Nagai T, Okuda H, Oh S S, Hojo M, Tanaka M, Sugano M and Osamura K 2003 Tensile damage and its influence on the critical current of Bi2223/Ag superconducting composite tape *Supercond. Sci. Technol.* **16** 988–94
[33] Shin H S and Katagiri K 2003 Critical current degradation behaviour in Bi-2223 superconducting tapes under bending and torsion strains *Supercond. Sci. Technol.* **16** 1012–8

[34] Fujii H, Garnier V, Giannini E and Flükiger R 2004 Effect of hot uniaxial pressing on the microstructure and critical current density of (Bi,Pb)-2223 tapes *Supercond. Sci. Technol.* **17** 263–8
[35] Takeda Y, Iwami T, Saito Y, Motoki T and Shimoyama J 2021 Fabrication of high Jc Bi2223 thick films through grain alignment technique using a permanent magnet *Physica C*.**584** 1353873
[36] Kametani F, Oloye T A, Jiang J, Osabe G and Kobayashi S 2019 Visualization of the grain structure in the filament cross sections of uniaxially textured high J_c Bi-2223 tapes *Appl. Phys. Express* **12** 093002